Reconstruction of the axis position and primary particle energy of extensive air showers in the SPHERE-2 experiment

Extended abstract

Vaiman Igor, SINP MSU

Introduction

Cosmic rays (CR) are highly energetic charged particles that traverse space. They play a crucial role in understanding the dynamics of space systems. Their energy spectrum spans 12 orders of magnitude (10^9 to 10^{21} eV), providing insights into their origin and propagation within the Solar System, Galaxy, and Metagalaxy. Above 10^{15} eV, indirect methods are employed to study cosmic rays through the detection of extensive air showers (EAS), utilizing Earth's atmosphere as a giant calorimeter.

The SPHERE-2 experiment focuses on detecting EAS using the relatively novel method of reflected Cherenkov light. This work enhances the experiment's data processing by incorporating a deeper understanding of the SPHERE-2 detector gained in recent years. The key improvement lies in modeling the detector as a stochastic system, enabling accurate estimation of instrumental uncertainties. Bayesian statistics serves as the primary mathematical framework for the analysis.

1 SPHERE-2 experiment

1.1 Method of reflected Cherenkov light to detect extensive air showers

Cherenkov light is a valuable tool for studying extensive air showers (EAS) due to its weak dependence on high-energy hadronic interaction models. The traditional direct detection method, similar to charged particle detection, employs ground array of detectors distributed over a large area to point-measure flux density.

However, unlike charged particles, Cherenkov light in the optical and near-optical range can be effectively scattered by the Earth's (for example, snow) surface and observed from above. The method of registering reflected light was first proposed by A. E. Chudakov [Chudakov1972] and further developed in the SPHERE-1 and SPHERE-2 experiments [1, 2].

One of the main advantages of this method is the access to Cherenkov light from the paraxial region of the shower, made possible by the extended fields of view of individual sensitive elements of the detector.

1.2 SPHERE-2 detector

1.2.1 Geometry

The SPHERE-2 detector was lifted by a balloon and suspended at an altitude ranging from 400 to 900 m. It utilized an optical system comprising a diaphragm, a spherical mirror, and a mosaic of photomultiplier tubes (PMTs) to collect Cherenkov light from EAS reflected by the snow surface below. Each PMT collected reflected light from an area with a diameter ranging from 10 to 50 m,

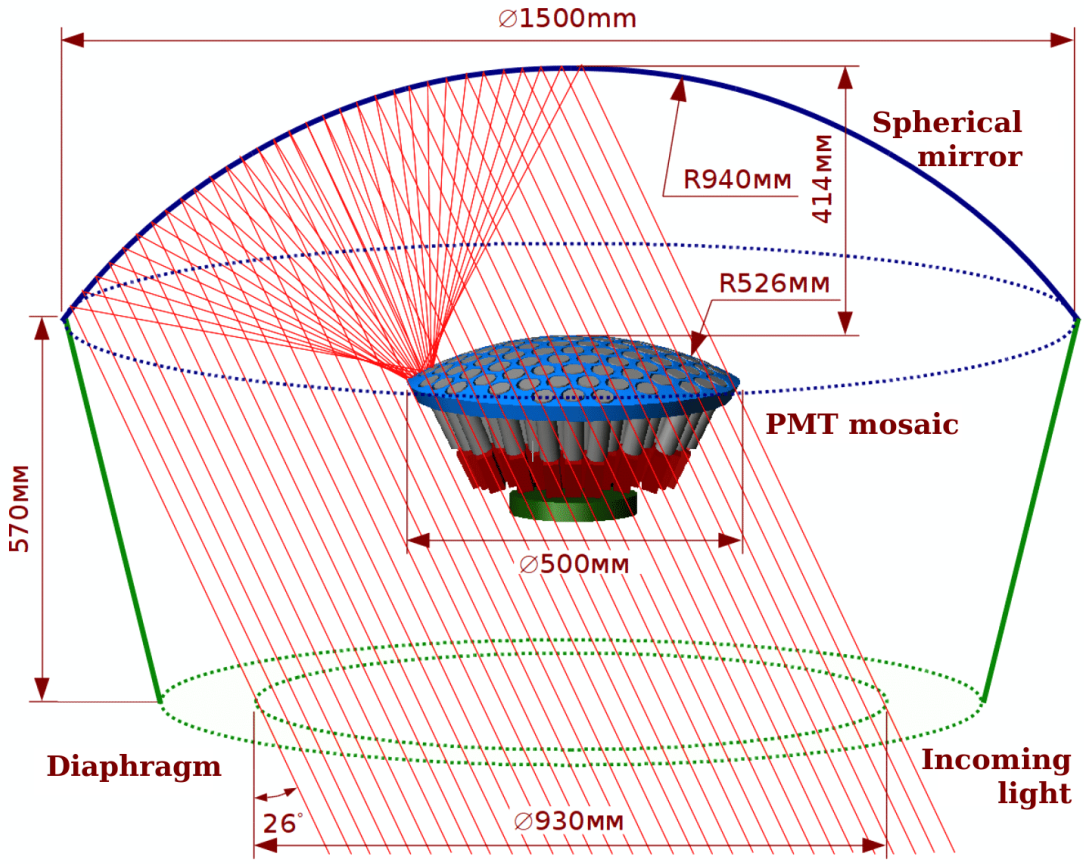

Figure 1.1: SPHERE-2 detector optical scheme

depending on the detector altitude. Figure 1.1 illustrates the optical scheme of the SPHERE-2 detector.

The PMT mosaic, arranged in an approximately hexagonal grid, was located near the focal surface of the spherical mirror. It consisted of 109 PMTs, with the central PMT being the Hamamatsu R3886, serving as a reference for detector calibration [3], and the remaining PMTs being Soviet-made PMT 84-3.

1.2.2 Intermediate PMT mode

When light strikes the PMT photocathode, it emits a photoelectron with a certain probability. This photoelectron then triggers a cascade of secondary photoelectrons through the dynode system, resulting in an observable charge at the anode.

The electron cascade within a PMT is a fundamentally stochastic process, as verified by direct laboratory measurements of anode charge fluctuations [3, Fig. 9]. Each dynode undergoes random multiplication, and due to the cascading nature, small variations in the early stages can lead to significant differences in amplification.

The stochastic nature of PMT amplification is not apparent when measuring high fluxes due to averaging. Likewise, it is not significant at low fluxes when the PMT operates in photon counting mode, allowing for the observation of well-resolved individual pulses. However, in the SPHERE-2 detector, PMTs operate in an intermediate mode: the flux is too high to resolve individual photons, yet insufficient for effective averaging. Consequently, the deconvolution problem needs to be formulated in statistical terms.

2 Bayesian deconvolution

Early stages of the SPHERE-2 analysis attempted to directly estimate the parameters of EAS photons in each PMT (photon count and arrival time distribution) from the recorded signal. However, this approach was unsuccessful due to various reasons. Instead, the idea emerged to perform a complete deconvolution, extracting information about the photon flux at the input of each PMT for every moment in time. This deconvolution process must consider the stochastic properties of the PMT. Similar problems are addressed in other domains, such as spectral measurements [4] and image processing [5], where Bayesian statistics proves to be valuable by interpreting probability as a measure of information or confidence in the value of a random variable [6].

2.1 Problem setup

The input signal is a set of δ-functions offsetted in time. We use detector's natural time bins (12.5 sec) and assume that within each time bin, δ-functions are distributed almost uniformly. Considering N time bins, our goal is to determine the photon count, denoted as n_i, in each time bin $[i-1, i]$ for $i = 1 \dots N$.

We assume that the PMT behaves as a linear system with a stochastic impulse response function $\tilde{h}(t)$. Each δ-function in the input signal is convolved with an independent sample $h(t) \sim \tilde{h}(t)$. This represents the idea of independent fluctuations in PMT amplification for each electron cascade. We assume that each sample from $\tilde{h}(t)$ is causal ($h(t) = 0$ for $t < 0$) and finite in time ($\exists \tilde{L}$ such that $h(t)(t) = 0,\ t > \tilde{L}$). We refer to this random function, which provides a new sample for each input δ-function, as the system's randomized impulse response (RIR). The problem of statistical deconvolution is formulated in Bayesian terms:

> Given the randomized impulse response of the system $\tilde{h}(t)$ and the output signal $s_j,\ j = 1, \dots, N + L$, find the posterior probability density functions for the values n_i, $i = 1, \dots, N$.

We use uninformative prior $P(\vec{n}) = Const$ and denote likelihood function $\mathcal{L}(\vec{s}, \vec{n}) = P(\vec{s}|\vec{n})$, which yields

$$P(\vec{n}|\vec{s}) = \frac{P(\vec{s}|\vec{n})\, P(\vec{n})}{P(\vec{s})} \propto \mathcal{L}(\vec{s}, \vec{n}) \tag{2.1}$$

2.2 Likelihood function

The PMT output signal $\vec{s}$ is a sample from a multivariate random variable. Denoting it as $\vec{S}$, we can express S_j it as:

$$S_j = \sum_{l=0}^{L} C(n_{j-l}, l) \tag{2.2}$$

$C(n, l)$ is a random variable that describes the contribution of n δ-functions with a delay of l bins. Here we take use RIR constraints.

To study the distribution of $C(n, l)$, Monte Carlo simulations are be employed. By sampling the RIR $h_k(t) \sim \tilde{h}(t)$ and an in-bin time $t_{\text{inbin}} \sim U(0, 1)$, we obtain a sample from $C(1, l) = h_k(l + 1 - t_{\text{inbin}})$. Adding n independent samples from it yields a sample from $C(n, l)$.

Directly sampling S_j to calculate likelihood of a particular $\vec{s}$ is computationally infeasible. We approximate the likelihood function using a multivariate normal distribution. We find this approximation suitable for input intensities as low as 4-5 δ-functions per bin, which corresponds to the background intensity observed in the SPHERE-2 detector.

The general form of multivariate normal distribution is

$$p(\vec{s}) = \left((2\pi)^{N+L} \det \Sigma\right)^{-1/2} \exp\left(-\frac{1}{2}(\vec{s} - \vec{\mu})^T \Sigma^{-1} (\vec{s} - \vec{\mu})\right) \tag{2.3}$$

The mean vector $\vec{\mu}$ and the covariance matrix Σ depend on the input $\vec{n}$ and the RIR $\tilde{h}(t)$. Specifically, $\vec{\mu} \equiv \mathbb{E}\vec{S}$ can be obtained from 2.2 by computing mean of left and right terms and using linearity. The matrix Σ can be expressed in terms of $C(n, l)$ autocovariance:

$$\Sigma_{ij} = \operatorname{cov}(S_i, S_j) = \sum_{l=0}^{L-(i-j)} \operatorname{cov}(C(n_{i-l}, l), C(n_{i-l}, l + (i - j))) \tag{2.4}$$

2.3 Discretization error

This approximation assumes precise measurement of the output signal. In reality, the output signal is discretized by ADC. We assume that the ADC rounds down its input, i.e. for each recorded s_j, the actual input value lies somewhere between s_j and $s_j + \delta$, following a uniform distribution. To account for this error, we numerically integrate the likelihood function defined by 2.3

over an N-dimensional cube with side length δ and a lower corner positioned at $\vec{s}$:

2.4 Posterior distribution sampling

Using the obtained likelihood function $\mathcal{L}$, we estimate $\vec{n}$ based on the recorded output signal $\vec{s}$ and RIR $\tilde{h}(t)$. Employing Markov Chain Monte Carlo (MCMC) sampling [9], we draw a large sample from $P(\vec{n}|\vec{s}) \propto \mathcal{L}(\vec{n}, \vec{s})$. From this sample of potential $\vec{n}$ values, we obtain the best-fitting input value for the system and its associated error.

For this study, we utilize the affine-invariant MCMC method [10] implemented in the Python package emcee [11].

2.5 Deconvolution results

We illustrate deconvolution procedure on toy input data: Poisson background with mean $\lambda = 20$ photons per time bin and a «signal» photon packet: 3 bins with additional Poisson signal with $\lambda_{\text{signal}} = 40$. Fig. 2.1 illustrates the system's input and output on the top panel and the deconvolution results on the bottom panel.

3 Extensive air shower parameters estimation

3.1 Shower photon packets

After deconvolution, our goal is to identify EAS photons among the background. These photons are expected to arrive in "packets" with a normal distribution of arrival times, characterized by parameters n_{EAS} (total number of photons), μ_t (mean arrival time), and σ_t (arrival time standard deviation). The background,

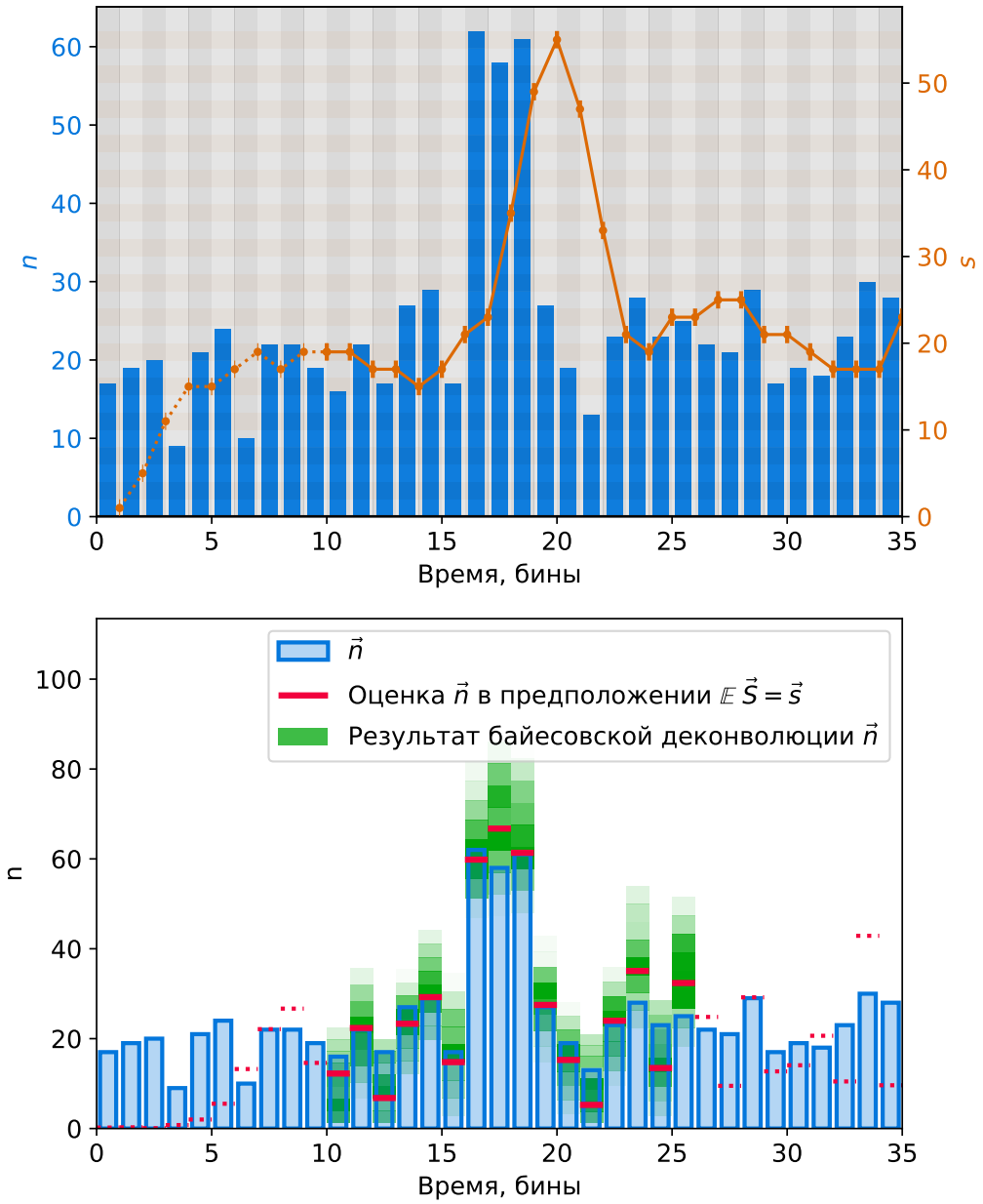

Figure 2.1: Bayesian deconvolution performed on toy input data. Top panel: toy input data $\vec{n}$ (blue) and corresponding system's output (convolution with SPHERE-2 randomized impulse response) $\vec{s}$, orange (X axis: «Time, bins»). Bottom pannel: same input data $\vec{n}$ (blue); rough $\vec{n}$ estimation from mean values, MCMC sampling starting point (red); deconvolution result, marginal posterior distributions in each time bin (green).

composed of starlight and zodiacal light reflected from the snow, follows a Poisson distribution with mean λ_n known from calibration.

We approach this as a Bayesian problem, seeking the posterior distribution of EAS photon packet parameters based on the distribution for $\vec{n}$ obtained from deconvolution.

The likelihood function is calculated by sampling signal, subtracting it from the $\vec{n}$ and calculating Poisson likelihood for the remaining background signal.

After that, we use similar MCMC technique to get the final signal reconstruction result: posterior distribution of photon packet parameters. Performing both steps of the analysis within the same Bayesian framework lets us effectively chain these two analysis together, while also keeping them separate.

We can also use Bayesian information criterion (BIC) [13] to calculate the significance of EAS signal in each channel. We use it to remove background-only channels from further analysis.

Figure 3.1 shows an example of full EAS photon packet parameters reconstruction for an experimental event.

3.2 Shower parameter reconstruction

The rest of the reconstruction performed here in this work standard methods, with the exception of being applied to the output of Bayesian reconstruction.

- Shower arrival direction is determined by a plain fit of arrival times. Ground level arrival times for each channel are determined from μ_t by subtracting ground-to-detector light travel time, accounting for the detector altitude and inclination.

- Shower axis position is determined by finding a point on the surface that maximizes the probability (with respect to each channel's posterior distribution) of monotonously decreasing lateral distribution function.

- Lateral distribution function for EAS Cherenkov light is determined by fitting a parametrized function to the data. In this work, a simplified LDF

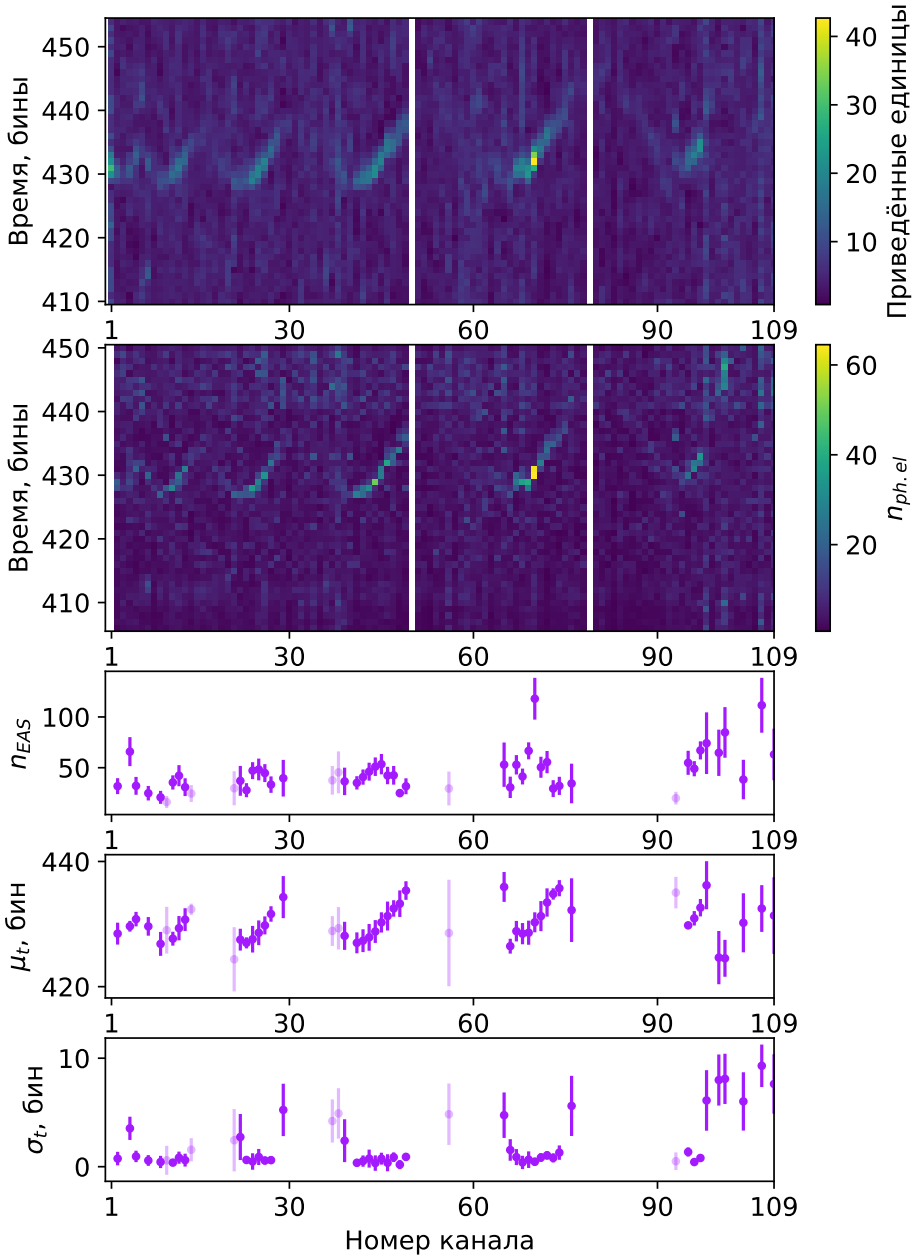

Figure 3.1: Full signal reconstruction for experimental event #10675. Common X axis: channel number, see [3] for numbering scheme. Top panel: experimental data with calibration coefficiens applied. Second-to-top panel: deconvolution output, photon count in each time bin. Three bottom panels: reconstructed photon packet parameters n_{EAS}, μ_t, σ_t — dots and error bars represent marginal means and standard deviations; dimmed values are signals with $\Delta\text{BIC} \in (0, 4]$, negative ΔBIC (background-only channels) are omitted.

from [16] is used. The fitting is done by convolving the LDF with each channel's light collection function (which is calculate from detector's optic system model). Shower energy is then derived from LDF parameters.

Bibliography

[1] R.A. Antonov et al. "Primary cosmic ray spectrum measured using Cherenkov light reflected from the snow surface". In: Nuclear Physics B - Proceedings Supplements 52.3 (Feb. 1997), pp. 182–184. DOI: 10.1016/s0920-5632(96)00876-6.

[2] R. A. Antonov et al. "Balloon-Borne measurements of the CR energy spectrum in the energy range 10^{16}-10^{17} EV". In: International Cosmic Ray Conference. Vol. 1. International Cosmic Ray Conference. Jan. 2001, p. 59.

[3] R.A. Antonov et al. "The LED calibration system of the SPHERE-2 detector". In: Astroparticle Physics 77 (Apr. 2016), pp. 55–65. DOI: 10.1016/j.astropartphys.2016.01.004.

[4] Cynthia Rhode and Scott Whittenburg. "Bayesian Deconvolution". In: Spectroscopy Letters 26.6 (July 1993), pp. 1085–1102. DOI: 10.1080/00387019308011596.

[5] David Wipf and Haichao Zhang. "Revisiting Bayesian Blind Deconvolution". In: arXiv e-prints, arXiv:1305.2362 (May 2013), arXiv:1305.2362. arXiv: 1305.2362 [cs.CV].

[6] Andrew Gelman et al. Bayesian Data Analysis. Chapman and Hall/CRC, Nov. 2013. DOI: 10.1201/b16018.

[7] Alan Genz. “Numerical Computation of Multivariate Normal Probabilities”. In: Journal of Computational and Graphical Statistics 1.2 (June 1992), pp. 141–149. DOI: 10.2307/1390838.

[8] Pauli Virtanen et al. “SciPy 1.0: Fundamental Algorithms for Scientific Computing in Python”. In: Nature Methods 17 (2020), pp. 261–272. DOI: 10.1038/s41592-019-0686-2.

[9] Sanjib Sharma. “Markov Chain Monte Carlo Methods for Bayesian Data Analysis in Astronomy”. In: Annual Review of Astronomy and Astrophysics 55.1 (Aug. 2017), pp. 213–259. DOI: 10.1146/annurev-astro-082214-122339.

[10] Jonathan Goodman and Jonathan Weare. “Ensemble samplers with affine invariance”. In: Communications in Applied Mathematics and Computational Science 5.1 (Jan. 2010), pp. 65–80. DOI: 10.2140/camcos.2010.5.65.

[11] Daniel Foreman-Mackey. “corner.py: Scatterplot matrices in Python”. In: The Journal of Open Source Software 1.2 (June 2016), p. 24. DOI: 10.21105/joss.00024.

[12] R.A. Antonov et al. “The SPHERE-2 detector for observation of extensive air showers in 1 PeV – 1 EeV energy range”. In: Astroparticle Physics 121 (Sept. 2020), p. 102460. DOI: 10.1016/j.astropartphys.2020.102460.

[13] Gideon Schwarz. “Estimating the Dimension of a Model”. In: The Annals of Statistics 6.2 (Mar. 1978). DOI: 10.1214/aos/1176344136.

[14] H. Akaike. “A new look at the statistical model identification”. In: IEEE Transactions on Automatic Control 19.6 (Dec. 1974), pp. 716–723. DOI: 10.1109/tac.1974.1100705.

[15] Robert E. Kass and Adrian E. Raftery. “Bayes Factors”. In: Journal of the American Statistical Association 90.430 (June 1995), pp. 773–795. DOI: 10.1080/01621459.1995.10476572.